

ORIGINAL ARTICLE

Uncoupling DAPK1 from NMDA receptor GluN2B subunit exerts rapid antidepressant-like effects

S-X Li^{1,2,9}, Y Han^{1,2,3,9}, L-Z Xu^{1,2,3,4,9}, K Yuan^{4,5,6}, R-X Zhang^{1,2,4}, C-Y Sun^{1,2,4}, D-F Xu⁴, M Yuan^{1,2,3}, J-H Deng⁴, S-Q Meng^{1,2}, X-J Gao^{1,2,3,4}, Q Wen⁷, L-J Liu^{1,2}, W-L Zhu^{1,2}, Y-X Xue^{1,2}, M Zhao⁸, J Shi^{1,2} and L Lu^{1,2,4,5,6}

Several preclinical studies have reported the rapid antidepressant effects of *N*-methyl-D-aspartate receptor (NMDAR) antagonists, although the underlying mechanisms are still unclear. Death-associated protein kinase 1 (DAPK1) couples GluN2B subunits at extrasynaptic sites to regulate NMDAR channel conductance. In the present study, we found that chronic unpredictable stress (CUS) induced extracellular glutamate accumulation, accompanied by an increase in the DAPK1–NMDAR interaction, the high expression of DAPK1 and phosphorylated GluN2B at Ser1303, a decrease in phosphorylated DAPK1 at Ser308 and synaptic protein deficits in the rat medial prefrontal cortex (mPFC). CUS also enhanced GluN2B-mediated NMDA currents and extrasynaptic responses that were induced by bursts of high-frequency stimulation, which may be associated with the loss of astrocytes and low expression of glutamate transporter-1 (GLT-1). The blockade of GLT-1 in the mPFC was sufficient to induce depressive-like behavior and cause similar molecular changes. Selective GluN2B antagonist, DAPK1 knockdown by adeno-associated virus-mediated short-hairpin RNA or a pharmacological inhibitor, and the uncoupling of DAPK1 from the NMDAR GluN2B subunit produced rapid antidepressant-like effects and reversed CUS-induced alterations in the mPFC. The inhibition of DAPK1 and its interaction with GluN2B subunit in the mPFC also rescued CUS-induced depressive-like behavior 7 days after treatment. A selective GluN2B antagonist did not have rewarding effects in the conditioned place preference paradigm. Altogether, our findings suggest that the DAPK1 interaction with the NMDAR GluN2B subunit acts as a critical component in the pathophysiology of depression and is a potential target for new antidepressant treatments.

Molecular Psychiatry (2018) **23**, 597–608; doi:10.1038/mp.2017.85; published online 25 April 2017

INTRODUCTION

Depression is one of the most prevalent and debilitating mental disorders, causing significant disability and affecting more than 350 million people worldwide.^{1,2} A major limitation of current pharmacotherapies for depression is that the drugs typically take weeks or months to produce a therapeutic response, highlighting the pressing need to develop rapidly acting antidepressants. Accumulating evidence implicates the glutamatergic system in the pathophysiology and treatment of depression. Glutamate levels are elevated in patients with major depressive disorders and in rodents after chronic unpredictable stress (CUS),^{3–5} which may result from the loss and dysfunction of astrocytes.⁶ Extracellular glutamate accumulation can trigger the excessive activation of glutamatergic receptors and precipitate excitotoxicity.⁷ Preclinical studies also showed that various *N*-methyl-D-aspartate receptor (NMDAR) antagonists induce a rapid increase in synaptic glutamate release, with the activation of glutamate transmission and recycling into glia, rather than glutamate accumulation in the extrasynaptic space, in the rat medial prefrontal cortex (mPFC),⁸ producing rapid antidepressant-like effects.^{9–11} A better understanding of glutamatergic dysregulation in major depressive

disorders is important for providing mechanistic insights and identifying new therapeutic targets.

NMDARs are heterooligomeric complexes that are composed of an essential GluN1 subunit, combined with regulatory GluN2 (GluN2A–D) subunits and, in some cases, GluN3 (GluN3A–B) subunits.¹² GluN2A- and GluN2B-containing NMDARs are considered the major isoforms of functional NMDARs in neurons.¹³ GluN2A-containing NMDARs are mainly located in synapses and preferentially mediate cell survival. GluN2B-containing NMDARs mainly reside at extrasynaptic sites and are involved in cell death.^{14–16} The detrimental roles of the GluN2B subunit have been implicated in many central nervous system disorders, including Alzheimer's disease, Huntington's disease and ischemia.^{15,17–20} Genetic deletion or the pharmacological inhibition of the GluN2A and GluN2B subunits produces antidepressant-like effects in rodents.^{21–24} Selective GluN2B antagonism also produces an antidepressant response in patients with treatment-resistant major depressive disorder.^{25,26} However, still unknown are the precise mechanisms by which the selective blockade of GluN2B-containing receptors produces rapid antidepressant effects.

¹National Institute on Drug Dependence, Peking University, Beijing, China; ²Beijing Key Laboratory of Drug Dependence, Peking University, Beijing, China; ³Department of Pharmacology, School of Basic Medical Sciences, Peking University Health Science Center, Beijing, China; ⁴Peking University Sixth Hospital, Peking University Institute of Mental Health, Key Laboratory of Mental Health, Ministry of Health (Peking University), National Clinical Research Center for Mental Disorders (Peking University Sixth Hospital), Beijing, China; ⁵Peking-Tsinghua Center for Life Sciences, Peking University, Beijing, China; ⁶PKU-IDG/McGovern Institute for Brain Research, Peking University, Beijing, China; ⁷Wuhan University School of Pharmaceutical Sciences, Wuhan, China and ⁸Key Lab of Mental Health, Institute of Psychology, Chinese Academy of Sciences (MZ), Beijing, China. Correspondence: Professor L Lu, Peking University Sixth Hospital, Peking University Institute of Mental Health, Key Laboratory of Mental Health, Ministry of Health (Peking University), National Clinical Research Center for Mental Disorders (Peking University Sixth Hospital), 51 Huayuan Bei Road, Haidian District, Beijing 100191, China. E-mail: linlu@bjmu.edu.cn

⁹These authors contributed equally to this work.

Received 16 June 2016; revised 23 February 2017; accepted 28 February 2017; published online 25 April 2017

Under physiological conditions, negative feedback regulation prevents intracellular calcium overload.²⁷ Under pathological conditions, the overstimulation of NMDARs results in excessive calcium influx and excitotoxicity. Death-associated protein kinase 1 (DAPK1) belongs to a family of calcium/calmodulin-dependent protein kinases. Recent studies revealed that activated DAPK1 directly binds to and phosphorylates the GluN2B subunit at Ser1303 to regulate NMDAR channel conductance at extrasynaptic sites.¹⁹ Extrasynaptic NMDAR stimulation triggers the cyclic AMP response element-binding protein (CREB) shut-off pathway, which consequently reduces brain-derived neurotrophic factor (BDNF) expression.^{14,17,28} We hypothesized that the DAPK1 interaction with the GluN2B subunit in response to extracellular glutamate accumulation has a critical role in the pathophysiology of depression, and targeting this process could be a practical strategy for developing novel antidepressants.

The present study investigated the mechanisms by which DAPK1 coupling to the GluN2B subunit contributes to the development of depressive-like behavior. We assessed the effects of CUS on extracellular glutamate levels and GluN2B-associated signaling molecules in the mPFC. Under conditions of stress, extracellular glutamate overflows onto extrasynaptic GluN2B-containing NMDARs, enhancing their interaction with activated DAPK1 and leading to decreases in CREB activity and BDNF expression. We found that targeting these key connections produced rapid and sustained antidepressant-like effects and reversed stress-induced alterations in the mPFC.

MATERIALS AND METHODS

Animals

Male Sprague–Dawley rats (240–260 g) were housed under a reverse 12 h/12 h light/dark cycle with free access to food and water.

Drugs

Ifenprodil tartrate (Sigma-Aldrich, St. Louis, MO, USA) was dissolved in 5% dimethylsulfoxide and 9% Tween 80/saline before use.²⁹ Dihydrokainate (DHK; 6.25 nmol μl^{-1} ; Sigma-Aldrich) was dissolved in 0.01 M phosphate-buffered saline (pH 7.4).³⁰ TC-DAPK 6 (290 nm) was dissolved in 2% dimethylsulfoxide and phosphate-buffered saline (pH 7.4).³¹ Both Tat-GluN2B_{CT} and Tat-sGluN2B_{CT} were dissolved in saline.¹⁹ Ketamine hydrochloride (10 mg kg^{-1}) was obtained from Jiangsu Hengrui Medicine (Lianyungang, Jiangsu, China) and dissolved in saline. PEAQX (5 mg kg^{-1}) and Ro 25–6981 (10 mg kg^{-1}) were purchased from Abcam (Cambridge, UK) and dissolved in saline.

Surgery

Guide cannulas were bilaterally implanted 1 mm above the mPFC (anterior/posterior, +3.2 mm; medial/lateral, ± 2.0 mm; and dorsal/ventral, -2.8 mm) at a 16° angle.³² See Supplementary Information for details.

Sucrose preference test and forced swim test

The procedures were based on previous studies.^{33,34} After adaptation for 48 h, the rats were deprived of water and food for 4 h and then subjected to the sucrose preference test, in which they were housed in individual cages for 1 h and had free access to two bottles that contained 1% sucrose or tap water. The forced swim test (FST) consisted of a plastic cylinder (25 cm diameter and 65 cm height) that was filled with water (45 cm depth) at a temperature of 23–25 °C. Immobility was defined as minimal movement of both the four limbs and tail of the rats.

CUS protocol

CUS was conducted with a variable sequence of different mild stressors, with two stressors per day for 28 days, which was adapted from previous studies.^{33,34}

In vivo microdialysis and liquid chromatography–mass spectrometry for glutamate quantification

Microdialysis cannulas were implanted unilaterally in the right mPFC (anterior/posterior, +3.2 mm; medial/lateral, ± 0.5 mm; and dorsal/ventral, -2.8 mm, 0° angle). The cannula was implanted 4 days before microdialysis. The rats were handled for 10 min per day before microdialysis. The microdialysis probe extended 1 mm below the microdialysis cannula (that is, directly in the mPFC). The procedure was based on previous studies.^{35,36} See Supplementary Information for details.

Tissue sample preparation, immunoprecipitation and western blot
The procedures were based on previous studies.^{19,37–39} See Supplementary Information for details.

Whole-cell recordings in acute brain slices

Layer V pyramidal neurons in the mPFC were targeted for slice recordings. NMDAR-mediated excitatory postsynaptic currents were pharmacologically isolated by bath-applying the α -amino-3-hydroxy-5-methyl-4-isoxazolepropionic acid receptor antagonist CNQX (10 μM) at a clamp voltage of +50 mV. The stimulation intensity was adjusted to evoke a 100 pA response. Data were collected and analyzed using AxoGraph X software (AxoGraph Scientific, Sydney, NSW, Australia). See Supplementary Information for details.

Statistical analysis

The data are expressed as mean \pm s.e.m. Rats were randomly allocated to treatment condition, and all of the data were collected randomly. The behavioral and biochemical/electrophysiological measurements were performed with the experimenter blind to the experimental groups. Statistical analysis of the data was performed using independent samples *t*-test, one-way analysis of variance (ANOVA), two-way ANOVA or two-way ANOVA for repeated measures followed by Tukey's *post hoc* test as appropriate. Values of $P < 0.05$ were considered statistically significant.

RESULTS

Chronic stress increased extracellular glutamate accumulation and caused glutamate overflow onto GluN2B-containing NMDARs in the mPFC

We used the CUS paradigm to assess the effects of chronic stress on extracellular glutamate levels in the mPFC. The rats were randomly divided into a CUS group and a control group, and subjected to 28 days of CUS exposure or handling, followed by tests of depressive-like behavior, *in vivo* microdialysis to determine extracellular glutamate levels and brain sample collection for the detection of astrocyte-specific markers (Figures 1a and d). Rats that were exposed to CUS exhibited a decrease in sucrose preference ($t_{20} = -3.119$, $P < 0.01$; Supplementary Figure S1b) and no changes in total fluid consumption (Supplementary Figure S1c) in the sucrose preference test and an increase in immobility time in the FST ($t_{20} = 3.076$, $P < 0.01$; Supplementary Figure S1d). *In vivo* microdialysis and high-performance liquid chromatography–mass spectrometry were performed to determine extracellular glutamate levels in the mPFC. Glutamate levels significantly increased in the mPFC in CUS-exposed rats (main effect of group: $F_{1,7} = 8.400$, $P < 0.05$; Figure 1c).

Astrocytes are crucial for glutamate uptake and metabolism in the central nervous system. CUS significantly decreased the expression of two astrocyte-specific markers in the PFC (glial fibrillary acidic protein, $t_{14} = 6.743$, $P < 0.01$; glutamate transporter-1, $t_{14} = 4.990$, $P < 0.01$; Figures 1e and f), and decreased the number of glial fibrillary acidic protein-positive cells per mm^2 ($t_6 = 4.433$, $P < 0.01$; Figures 1g and h), without affecting the number of NeuN-positive cells per mm^2 (Supplementary Figures S1e and f) in the mPFC. CUS increased NMDAR-mediated currents that were evoked by high-frequency stimulation, which was blocked by the GluN2B-specific antagonist ifenprodil (main effect of ifenprodil: $F_{1,20} = 4.561$, $P < 0.05$; Figure 1j and Supplementary Figure S3b). With the minimal stimulation protocol that activated a small

number of afferents and did not cause glutamate spillover, CUS did not affect the normalized NMDAR-mediated excitatory postsynaptic current amplitude (Supplementary Figure S2). In

addition, CUS did not alter the NMDA decay time that was evoked by a single pulse (Supplementary Figure S3a) but increased the NMDA decay time after bursts of high-frequency stimulation

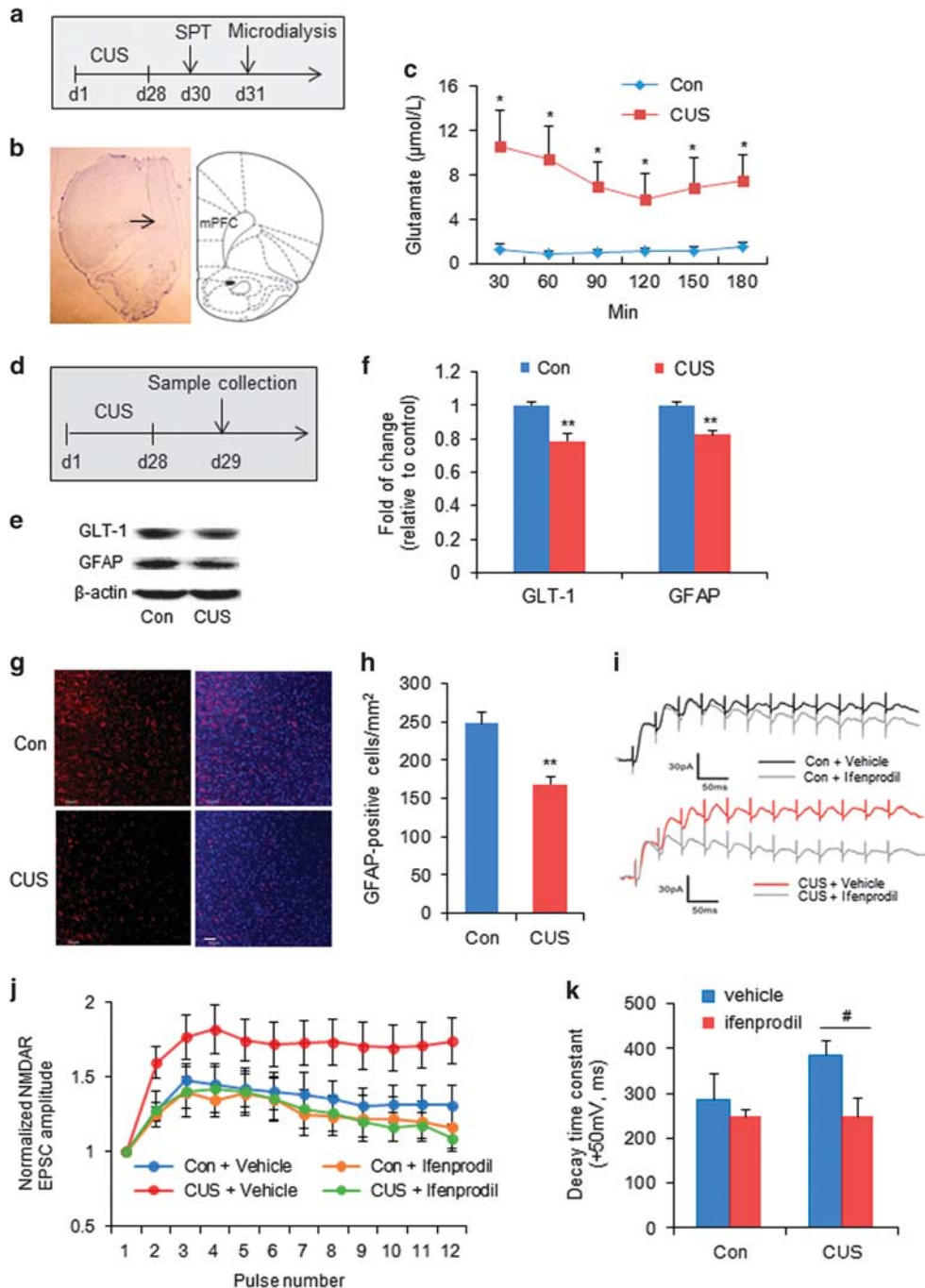
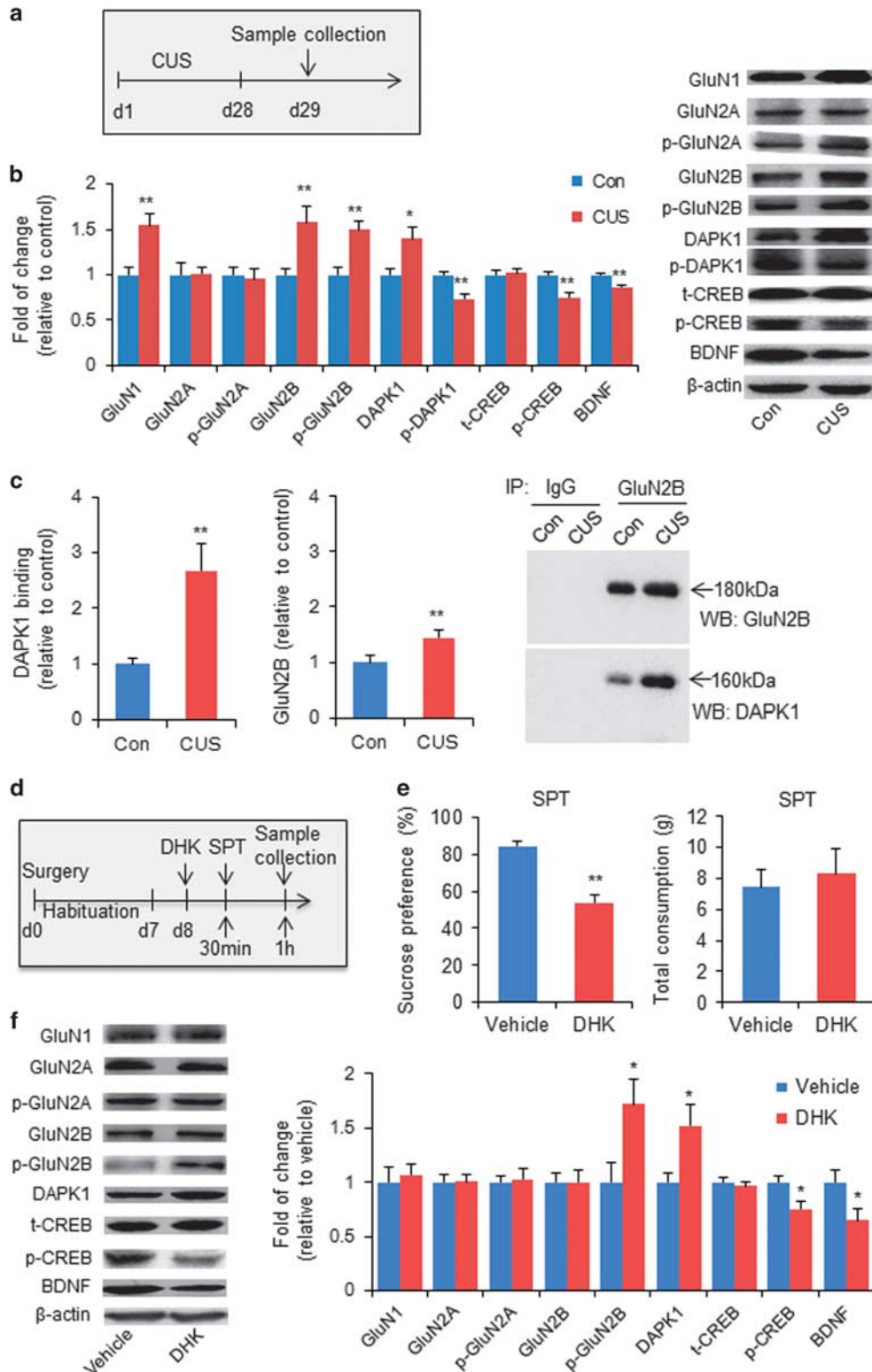


Figure 1. Chronic unpredictable stress increased extracellular glutamate levels and activated extrasynaptic GluN2B-containing NMDARs in the mPFC. **(a)** Timeline of CUS exposure, behavioral testing and microdialysis ($n=4-5$ per group). **(b)** Photograph of microdialysis site in the mPFC. **(c)** Extracellular glutamate in CUS-exposed rats was significantly higher than that in control rats. The levels of glutamate were measured every 30 min for 3 h after probe equilibration in the mPFC. **(d)** Timeline of CUS exposure and sample collection ($n=8$ per group). **(e, f)** Representative western blots and quantification of fold changes in GLT-1 and GFAP expression in the mPFC relative to control. **(g)** Representative image of GFAP-labeled astrocytes in the mPFC, counterstained with DAPI. Scale bar = 50 μm . **(h)** Results are expressed as mean \pm s.e.m. of GFAP-positive cells per mm^2 . $n=4$ per group. **(i)** Representative EPSC traces. **(j)** Plot of the normalized and averaged amplitudes of NMDAR EPSCs that were evoked at 40 Hz in the mPFC at a holding potential of +50 mV in the presence and absence of ifenprodil ($n=6$ neurons per group). **(k)** Average decay time constant of NMDAR EPSCs that were evoked by 12 pulses at 40 Hz stimulation in the presence and absence of ifenprodil. The data are expressed as mean \pm s.e.m., * $P < 0.05$, ** $P < 0.01$, compared with control group; # $P < 0.05$, compared with CUS+vehicle group. CUS, chronic unpredictable stress; DAPI, 4',6'-diamidino-2-phenylindole; EPSC, excitatory postsynaptic current; GFAP, glial fibrillary acidic protein; GLT-1, glutamate transporter 1; mPFC, medial prefrontal cortex; NMDAR, N-methyl-D-aspartate receptor.

($F_{1,20}=3.664$, $P=0.07$; Figure 1k), which may be attributable to synaptic glutamate overflow onto distal extrasynaptic GluN2B-containing NMDARs that prolongs the excitatory postsynaptic current decay time.^{40,41} We speculate that CUS-induced astrocyte dysfunction produced glutamate overflow and accumulation in the mPFC, activating extrasynaptic GluN2B-containing NMDARs and ultimately leading to depressive-like behavior.

Chronic stress and blockade of glutamate uptake overactivated GluN2B-containing NMDARs and inhibited the CREB–BDNF pathway in the mPFC

We then tested the effects of chronic stress on NMDAR subunits and associated signaling molecules in the mPFC. CUS increased the levels of GluN1 ($t_{15}=-3.464$, $P<0.01$), GluN2B ($t_{15}=-3.104$, $P<0.01$), phosphorylated GluN2B (p-GluN2B) at Ser1303



($t_{15} = -3.662$, $P < 0.01$) and DAPK1 ($t_{15} = -2.767$, $P < 0.05$), and decreased the levels of p-DAPK1 at Ser308 ($t_{15} = 4.633$, $P < 0.01$), p-CREB ($t_{15} = 3.832$, $P < 0.01$) and BDNF ($t_{15} = 4.107$, $P < 0.01$) in the mPFC (Figure 2b). The levels of GluN2A, p-GluN2A (Tyr1325) and total CREB (t-CREB) were unaffected by CUS (Figure 2b). Co-immunoprecipitation revealed an enhanced interaction between DAPK1 and the GluN2B subunit in the mPFC after chronic stress (DAPK1: $t_{10} = -3.654$, $P < 0.01$; GluN2B: $t_{10} = -3.429$, $P < 0.01$), which may explain the increase in p-GluN2B at Ser1303 (Figure 2c).

We further blocked astrocytic glutamate uptake by directly infusing the glutamate transporter-1 inhibitor DHK (6.25 nmol μl^{-1} ; 0.5 μl per side) in the mPFC, which rapidly decreased sucrose preference ($t_{15} = 6.678$, $P < 0.01$), without affecting total fluid consumption (Figure 2e). The levels of p-GluN2B ($t_{15} = -2.414$, $P < 0.05$) and DAPK1 ($t_{15} = -2.439$, $P < 0.05$) increased, whereas the levels of p-CREB ($t_{15} = 2.843$, $P < 0.05$) and BDNF ($t_{15} = 2.383$, $P < 0.05$) decreased in the mPFC in DHK-treated rats compared with vehicle-treated rats (Figure 2f). No significant changes were found in the levels of GluN1, p-GluN2A, GluN2A, GluN2B or CREB between groups (Figure 2f). DHK treatment did not affect the number of NeuN-positive cells per mm^2 (Supplementary Figures S1g and h) in the mPFC.

These results indicate that extracellular glutamate accumulation that was triggered by chronic stress enhanced the DAPK1–NMDAR interaction, induced overactivation of GluN2B-containing NMDARs and shut off the downstream CREB–BDNF pathway in the mPFC, which may contribute to the development of depressive-like behavior.

Selective blockade of GluN2B-containing NMDARs produced rapid antidepressant-like effects

Rats were intraperitoneally injected with the selective GluN2B antagonist ifenprodil at different doses (0.3, 1.0 and 3.0 mg kg^{-1} , intraperitoneal (i.p.)) and subjected to the open field test 30 min later, immediately followed by the FST (Supplementary Figure S4a). Ifenprodil at the three doses tested decreased immobility time in the FST ($F_{3,34} = 8.593$, $P < 0.01$) but did not affect locomotor activity in the open field test (Supplementary Figures S4b and c), indicating that ifenprodil has antidepressant-like effects in the FST. CUS decreased sucrose preference ($F_{4,43} = 10.370$, $P < 0.01$), without affecting total fluid consumption, and increased immobility time ($F_{4,43} = 5.463$, $P < 0.01$), both of which were rapidly and dose-dependently reversed by ifenprodil (Figures 3b and c, and Supplementary Figure S5b). Ifenprodil treatment did not affect CUS-induced depressive-like behavior 7 days after administration (Supplementary Figures S5d–f). Ifenprodil effectively rescued DHK-induced depressive-like behavior ($F_{1,28} = 15.125$, $P < 0.01$; Supplementary Figures S6b and c). These behavioral results indicate that selective blockade of the GluN2B subunit produced rapid antidepressant-like effects in the CUS paradigm and reversed depressive-like behavior that was induced by the blockade of astrocytic glutamate uptake.

We further explored the GluN2B subunit and associated signaling molecules in the mPFC after injecting a GluN2B antagonist. The rats were subjected to CUS or normal handling and injected with ifenprodil (3.0 mg kg^{-1} , i.p.). The brains were removed 30 min, 1 h and 6 h later for subsequent molecular analysis (Figure 3d). CUS increased the levels of p-GluN2B ($F_{4,41} = 4.486$, $P < 0.01$) and decreased the levels of p-CREB ($F_{4,41} = 5.368$, $P < 0.01$) and BDNF ($F_{4,41} = 6.825$, $P < 0.01$) in the mPFC, which were reversed by ifenprodil administration (Figure 3e). Ifenprodil did not affect CUS-induced increases in the levels of GluN1, DAPK1 or GluN2B in the mPFC (Figure 3e). CUS decreased the levels of synaptic proteins in the mPFC, including GluA1 ($F_{2,23} = 11.712$, $P < 0.01$), postsynaptic density 95 ($F_{2,23} = 6.768$, $P < 0.01$), and synapsin I ($F_{2,23} = 5.562$, $P < 0.05$), and these decreases were reversed by ifenprodil (Figure 3g).

Previous studies found that both the GluN2A and GluN2B subunits are involved in depressive-like behavior.^{21–23,42} We then investigated whether a selective GluN2A antagonist produces antidepressant-like effects in a model of CUS. Rats were subjected to CUS and administered the selective GluN2A antagonist PEAQX (5 mg kg^{-1} , i.p.), selective GluN2B-containing NMDAR antagonist Ro 25–6981 (10 mg kg^{-1} , i.p.) and nonselective NMDAR antagonist ketamine (10 mg kg^{-1} , i.p.). Ro 25–6981 and ketamine reversed the CUS-induced decrease in sucrose preference ($F_{4,56} = 7.102$, $P < 0.01$) and increase in immobility time ($F_{4,56} = 14.064$, $P < 0.01$). PEAQX at a dose of 5 mg kg^{-1} did not affect these behaviors (Supplementary Figure S7).

The conditioned place preference paradigm was used to assess whether the selective GluN2B antagonist ifenprodil has rewarding effects. Ifenprodil at doses of 0.3, 1.0 and 3.0 mg kg^{-1} did not induce significant conditioned place preference in rats (Supplementary Figure S8).

These results indicate that selective blockade of the GluN2B subunit had rapid antidepressant-like effects, and the selective GluN2B antagonist ifenprodil had no addiction potential.

DAPK1 inhibition in the mPFC prevented CUS-induced depressive-like behavior

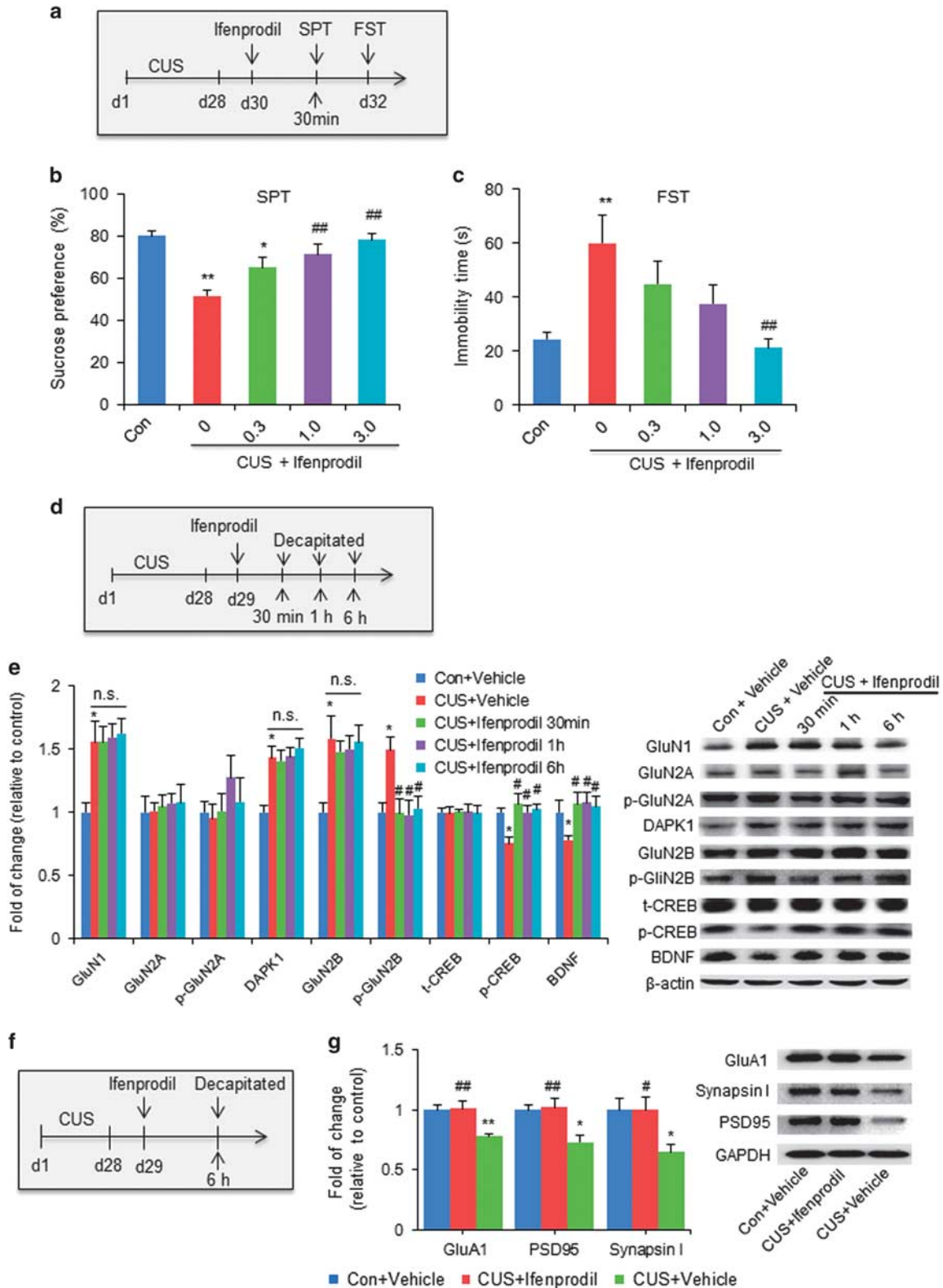
TC-DAPK 6 (290 nM; 0.5 μl per side), an inhibitor of DAPK1, was microinjected in the mPFC and reversed the CUS-induced decrease in sucrose preference ($F_{2,29} = 10.714$, $P < 0.01$; Supplementary Figure S9b), without affecting total fluid consumption (Supplementary Figure S9c), and reversed the increase in immobility time ($F_{2,29} = 28.406$, $P < 0.01$; Supplementary Figure S9d). These antidepressant effects lasted at least 7 days (sucrose preference test: $F_{2,28} = 6.297$, $P < 0.01$; FST: $F_{2,28} = 8.484$, $P < 0.01$; Supplementary Figures S9g–i). TC-DAPK 6 also reversed the CUS-induced increases in DAPK1 ($F_{2,29} = 5.235$, $P < 0.01$) and p-GluN2B ($F_{2,29} = 12.843$, $P < 0.01$), and reversed the CUS-induced decreases in p-CREB ($F_{2,29} = 6.531$, $P < 0.01$) and BDNF ($F_{2,29} = 6.806$, $P < 0.01$) in the mPFC (Supplementary Figure S9e).

Next, we further confirmed the effects of DAPK1 knockdown on depressive-like behavior. We first examined the efficiency of

Figure 2. Chronic unpredictable stress increased the expression levels of GluN2B and DAPK1 and their interaction in the mPFC. (a) Timeline of CUS exposure and sample collection ($n = 8–9$ per group). (b) Representative western blots and quantification of fold changes in GluN1, GluN2A, p-GluN2A, GluN2B, p-GluN2B, DAPK1, p-DAPK1, CREB, p-CREB and BDNF in the mPFC relative to control. (c) Co-immunoprecipitation of GluN2B with DAPK1 in the mPFC in control and CUS rats. The quantification analysis revealed a greater interaction between GluN2B and DAPK1 in the mPFC after CUS exposure ($n = 6$ per group). (d) Timeline of surgery, drug microinjection, behavioral testing and sample collection ($n = 8–9$ per group). (e) Microinjection of DHK in the mPFC rapidly decreased sucrose preference but did not affect total fluid consumption. (f) Representative western blots and quantification of fold changes in GluN1, GluN2A, p-GluN2A, GluN2B, p-GluN2B, DAPK1, CREB, p-CREB and BDNF in the mPFC after DHK infusion relative to vehicle. The data are expressed as mean \pm s.e.m. * $P < 0.05$, ** $P < 0.01$, compared with control or vehicle group. BDNF, brain-derived neurotrophic factor; CREB, cyclic AMP response element-binding protein; CUS, chronic unpredictable stress; DAPK1, death-associated protein kinase 1; DHK, dihydrokainate; mPFC, medial prefrontal cortex.

DAPK1 knockdown by adeno-associated virus (AAV)-mediated short hairpin RNA (Figure 4a). DAPK1 expression levels significantly decreased 3 weeks after the infusion of AAV-shDAPK1 in the mPFC ($t_{10}=9.737, P < 0.01$; Figure 4b). One week after infusing AAV-shDAPK1 or AAV-Scramble in the mPFC, the rats were

subjected to CUS and underwent behavioral tests (Figure 4c). The intra-PFC infusion of AAV-shDAPK1 prevented the CUS-induced decrease in sucrose preference ($F_{1,47}=8.751, P < 0.01$; Figures 4d and e) and prevented the CUS-induced increase in immobility time ($F_{1,47}=4.227, P < 0.05$; Figure 4f). The AAV-shDAPK1



microinjection decreased DAPK1 expression levels in both the control and CUS groups ($F_{1,28} = 4.148$, $P = 0.051$; Figure 4g). DAPK1 knockdown also reversed the CUS-induced increases in p-GluN2B (main effect of vector: $F_{1,28} = 13.302$, $P < 0.01$), and decreases in p-CREB ($F_{1,28} = 3.403$, $P = 0.076$) and BDNF ($F_{1,28} = 16.683$, $P < 0.01$) in the mPFC (Figure 4g), without affecting GluN1 or GluN2B levels.

These results indicate that DAPK1 knockdown or pharmacological inhibition significantly prevented or reversed CUS-induced depressive-like behavior, and normalized GluN2B signaling in the mPFC.

Uncoupling DAPK1 from the GluN2B subunit produces rapid and sustained antidepressant-like effects

Activated DAPK1 phosphorylates GluN2B subunits at Ser1303 and influences the activation of downstream signaling pathways. We examined whether the DAPK1–GluN2B interaction is directly involved in regulating depressive-like behavior. Uncoupling DAPK1 from the GluN2B subunit by Tat-GluN2B_{CT} infusion in the mPFC produced rapid antidepressant-like effects, reflected by an increase in sucrose preference ($F_{1,45} = 7.171$, $P = 0.01$; Figure 5b), no changes in total fluid consumption (Supplementary Figure S10b) and a decrease in immobility time ($F_{1,45} = 10.664$, $P < 0.01$; Figure 5c). Co-immunoprecipitation revealed that Tat-GluN2B_{CT} blocked the DAPK1–GluN2B interaction (DAPK1: $F_{1,28} = 9.680$, $P < 0.01$; GluN2B: $F_{1,28} = 0.071$, $P = 0.792$; Figure 5d). Tat-GluN2B_{CT} infusion in the mPFC also reversed the CUS-induced decrease in sucrose preference ($F_{1,41} = 5.704$, $P < 0.05$; Figure 5f), without affecting total fluid consumption (Supplementary Figure S10d), and reversed the CUS-induced increase in immobility time ($F_{1,41} = 15.619$, $P < 0.01$; Figure 5g) 7 days after administration.

These results indicate that inhibition of the DAPK1–GluN2B interaction in the mPFC produced rapid and sustained antidepressant-like effects.

DISCUSSION

In the present study, we found elevations in glutamate accumulation and astrocyte loss in the mPFC in CUS-exposed rats. Chronic stress also caused overactivation of GluN2B-containing NMDARs in the mPFC, with no abnormalities in GluN2A-containing NMDARs. Elevated glutamate accumulation that is induced by CUS or the blockade of glutamate uptake is critical for the development of depressive-like behavior by regulating the dynamics of the DAPK1–GluN2B subunit interaction and downstream CREB–BDNF pathway in the mPFC. The GluN2B antagonist rapidly reversed depressive-like behavior that was induced by CUS or the blockade of glutamate uptake, and normalized the levels of p-GluN2B (Ser1303), downstream signaling molecules (p-CREB and BDNF) and synaptic proteins in the mPFC. The inhibition of DAPK1 or its interaction with the NMDAR GluN2B subunit produced rapid and sustained antidepressant-like effects. We also found that the GluN2A

antagonist PEAQX at a dose of 5 mg kg⁻¹ had no effect on CUS-induced depressive-like behavior. Altogether, these results indicate that the DAPK1 interaction with the GluN2B subunit in the mPFC has an important role in the etiology of depression, and interfering with this process produces rapid and sustained antidepressant-like effects.

Extracellular glutamate concentrations are tightly regulated by glutamate transporters, especially glutamate transporter-1, which is predominantly expressed by astrocytes.⁴³ A loss of glial cells and lower expression of glutamate transporters in the PFC, amygdala and hippocampus were reported in clinical postmortem studies of depressed patients and animal models of depression.^{6,34,44–46} Similarly, we found astrocytes loss and the low expression of glutamate transporter-1 and glial fibrillary acidic protein in the mPFC after CUS, which may contribute to the persistently high levels of extracellular glutamate. We also found that the blockade of astrocytic glutamate uptake and CUS caused similar behavioral and molecular changes. These data support the hypothesis that glutamate-induced neurotoxicity contributes to the etiology of depression.^{3,47,48}

Accumulating evidence suggests that glutamatergic transmission via synaptic NMDARs (mainly GluN1-/GluN2A-containing NMDARs) promotes neuroprotection, whereas the stimulation of extrasynaptic NMDARs (mainly GluN1-/GluN2B-containing NMDARs) leads to excitotoxicity.^{49,50} Extrasynaptic NMDARs are activated by glutamate overflow from synapses or from the ectopic release of glutamate. Perturbations in the balance between synaptic and extrasynaptic NMDAR activity contribute to neuronal dysfunction in acute ischemia, Huntington's disease and Alzheimer's disease.^{15,18–20} We found that chronic stress did not alter synaptic NMDAR-mediated currents that were evoked by a single stimulation but increased NMDAR-mediated currents that were evoked by high-frequency stimulation, accompanied by a significant increase in the decay time of the receptor complex. The GluN2B-selective antagonist ifenprodil eliminated these alterations. Combined with the biochemical data that showed that CUS increased GluN2B but not GluN2A expression and activity in the mPFC, we speculate that a population of extrasynaptic GluN2B-containing NMDARs is activated by bursts of high-frequency stimulation under conditions of stress. A higher probability of presynaptic neurotransmitter release and glial dysfunction may also facilitate the overflow of glutamate to extrasynaptic sites,^{43,51} thus leading to the overactivation of extrasynaptic GluN2B-containing NMDARs. Altogether, excess extracellular glutamate after CUS can induce synaptic glutamate spillover, activate extrasynaptic GluN2B-containing NMDARs, trigger excitotoxicity and cell death pathways, and ultimately lead to neuronal atrophy and overall synaptic depression in the PFC and hippocampus and the development of depressive-like behaviors.^{6,52}

DAPK1 is a unique multidomain serine/threonine kinase, and its enzymatic activity is negatively regulated by autophosphorylation at Ser308 in the Ca²⁺/CaM regulatory domain.⁵³ We found that DAPK is dephosphorylated (Ser308) and activated after CUS, and activated DAPK1 is more likely recruited to bind with the GluN2B

Figure 3. GluN2B-specific antagonist produced rapid antidepressant-like effects and reversed CUS-induced synaptic protein deficits. **(a)** Timeline of CUS exposure, ifenprodil administration and behavioral testing ($n = 8–9$ per group). **(b, c)** Acute ifenprodil administration dose-dependently increased sucrose preference in the SPT **(b)** and reduced immobility time in the FST **(c)** in CUS-exposed rats. **(d)** Timeline of CUS exposure, ifenprodil injection and decapitation ($n = 8–10$ per group). **(e)** Representative western blots and quantification of fold changes in GluN1, GluN2A, p-GluN2A, GluN2B, p-GluN2B, DAPK1, CREB, p-CREB and BDNF in the mPFC 30 min, 1 h and 6 h after ifenprodil administration. **(f)** Timeline of CUS exposure, ifenprodil injection and decapitation ($n = 8–9$ per group). **(g)** Representative western blots and quantification of fold changes in GluA1, synapsin I and PSD95 in synaptoneurosomes in the mPFC 6 h after ifenprodil administration. The data are expressed as mean \pm s.e.m. * $P < 0.05$, ** $P < 0.01$, compared with control or control+vehicle group; # $P < 0.05$, ## $P < 0.01$, compared with CUS+vehicle group; n.s., nonsignificant difference. BDNF, brain-derived neurotrophic factor; CREB, cyclic AMP response element-binding protein; CUS, chronic unpredictable stress; DAPK1, death-associated protein kinase 1; FST, forced swim test; mPFC, medial prefrontal cortex; PSD95, postsynaptic density 95; SPT, sucrose preference test.

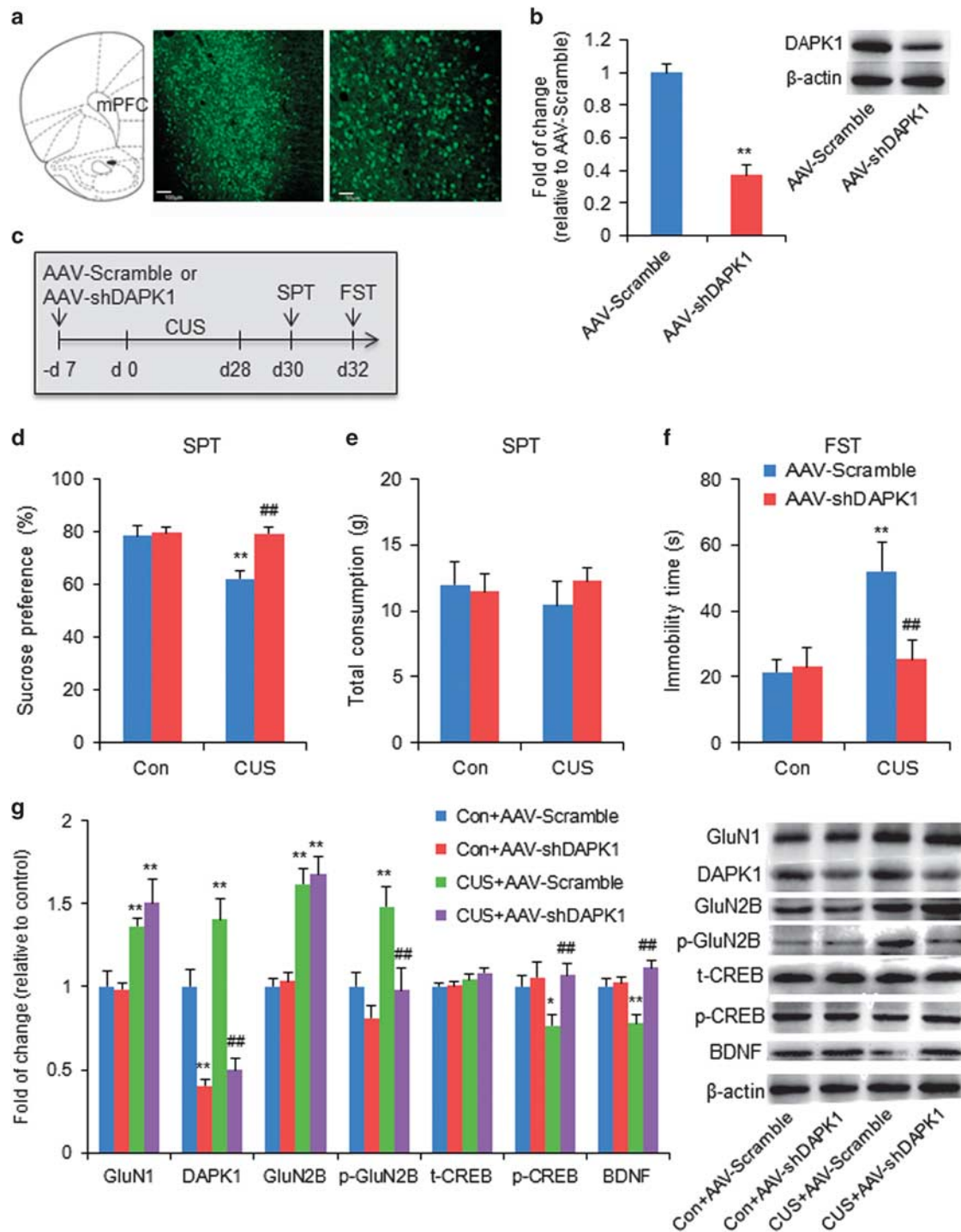


Figure 4. Knockdown of DAPK1 prevented CUS-induced depressive-like behavior and normalized GluN2B signaling in the mPFC. **(a)** Representative photographs of the injection sites and coronal brain sections in the mPFC. The figure shows representative micrographs of adeno-associated virus (AAV)-mediated enhanced green fluorescent protein (eGFP; green) after mPFC microinjection. Scale bars = 100 μ m (low-magnification images) and 50 μ m (high-magnification images). **(b)** DAPK1 expression in the mPFC in rats that were microinfused with AAV-Scramble or AAV-shDAPK1, quantified by western blot. ****** $P < 0.01$, compared with the AAV-Scramble group. $n = 6$ per group. **(c)** Timeline of AAV microinjection, CUS exposure and behavioral testing ($n = 8-18$ per group). **(d-f)** Intra-mPFC microinjection of AAV-shDAPK1 prevented the decrease in sucrose preference **(d)** and did not affect total fluid consumption **(e)** in the SPT, and prevented the increase in immobility time in the FST **(f)** induced by CUS. **(g)** Representative western blots and quantification of fold changes in GluN1, DAPK1, GluN2B, p-GluN2B, CREB, p-CREB and BDNF in the mPFC after AAV-Scramble or AAV-shDAPK1 microinjection ($n = 8$ per group). The data are expressed as mean \pm s.e.m. ***** $P < 0.05$, ****** $P < 0.01$, compared with control+AAV-Scramble group; **##** $P < 0.01$, compared with CUS+AAV-Scramble group. BDNF, brain-derived neurotrophic factor; CREB, cyclic AMP response element-binding protein; CUS, chronic unpredictable stress; DAPK1, death-associated protein kinase 1; FST, forced swim test; mPFC, medial prefrontal cortex; SPT, sucrose preference test.

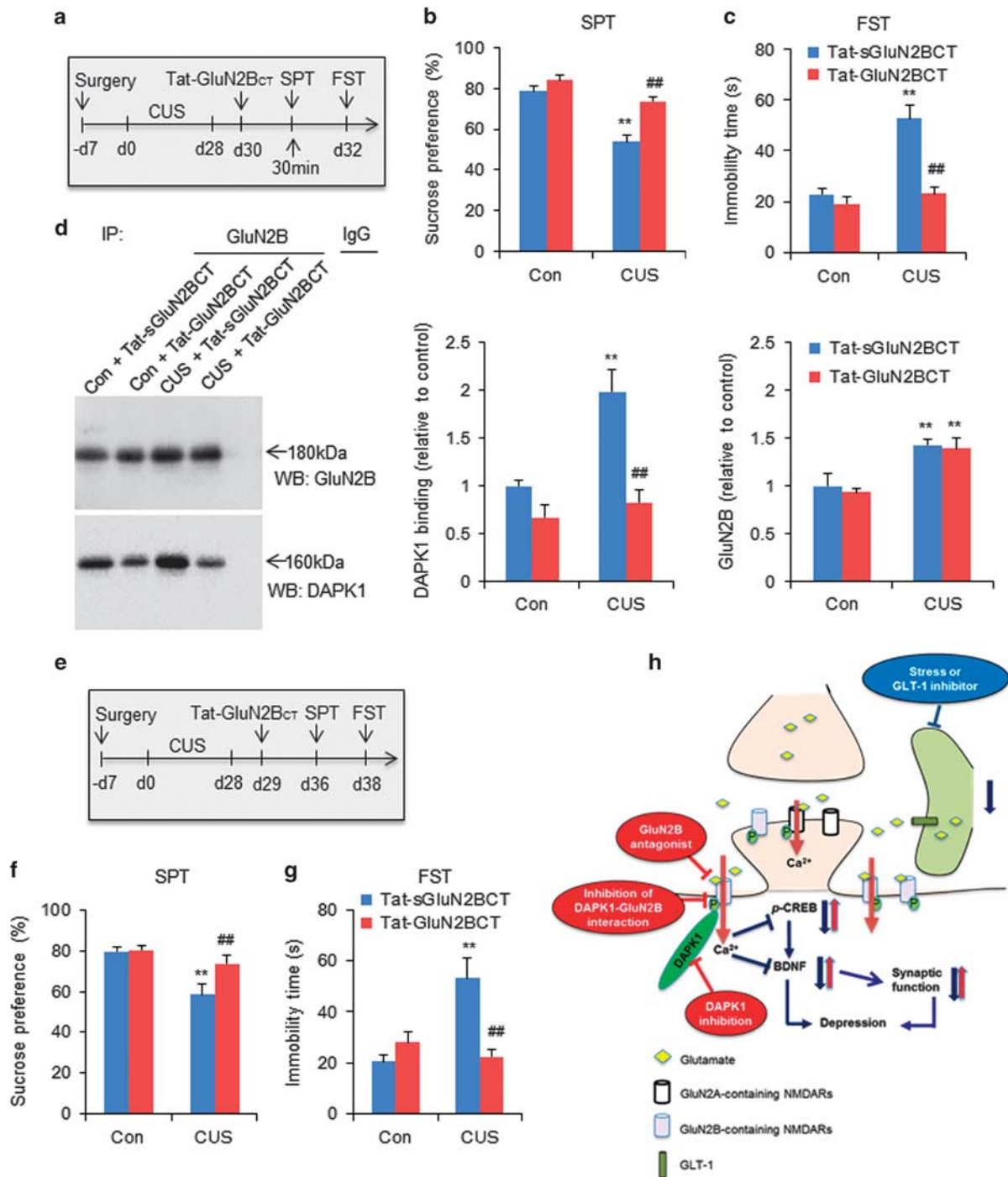


Figure 5. Inhibition of GluN2B–DAPK1 interaction produced rapid and sustained antidepressant-like effects. **(a)** Timeline of surgery, CUS exposure, drug microinjection and behavioral testing ($n=10–15$ per group). **(b, c)** Tat-GluN2B_{CT} rapidly increased sucrose preference in the SPT **(b)** and decreased immobility time in the FST **(c)** in CUS rats. **(d)** Representative GluN2B immunoprecipitation after Tat-GluN2B_{CT} and Tat-sGluN2B_{CT} treatment. Administration of Tat-GluN2B_{CT} led to the dissociation of GluN2B–DAPK1 complexes ($n=8$ per group). **(e)** Timeline of surgery, CUS exposure, drug microinjection and behavioral testing 7 days later ($n=10–13$ per group). **(f, g)** Tat-GluN2B_{CT} reversed the decrease in sucrose preference in the SPT **(f)** and the increase in immobility time in the FST **(g)** induced by CUS 7 days after administration. $^{**}P < 0.01$, compared with control+Tat-sGluN2B_{CT} group; $^{##}P < 0.01$, compared with CUS+Tat-sGluN2B_{CT} group. **(h)** Schematic diagram that illustrates the involvement of GluN2B-containing NMDARs and associated signaling molecules in the mPFC in depressive-like behavior. Chronic unpredictable stress exposure or the blockade of glutamate transporter-1 (GLT-1) impaired glutamate uptake into astrocytes, thus causing extracellular glutamate to accumulate and overflow onto extrasynaptic GluN2B-containing NMDARs. DAPK1 was activated when extracellular glutamate accumulated and phosphorylated GluN2B at Ser1303, leading to calcium influx. The activation of GluN2B by DAPK1 decreased p-CREB and BDNF levels and subsequently induced synaptic protein deficits and depressive-like behavior. Selective GluN2B antagonism, DAPK1 inhibition or uncoupling DAPK1 from the NMDAR GluN2B subunit rapidly rescued depressive-like behavior, followed by the normalization of GluN2B activation and increases in p-CREB and BDNF levels. GluN2B antagonism reversed the synaptic protein deficits that were caused by CUS exposure. BDNF, brain-derived neurotrophic factor; CREB, cyclic AMP response element-binding protein; CUS, chronic unpredictable stress; DAPK1, death-associated protein kinase 1; FST, forced swim test; mPFC, medial prefrontal cortex; NMDAR, *N*-methyl-D-aspartate receptor; SPT, sucrose preference test.

subunit and phosphorylates the GluN2B subunit at Ser1303. Elevated glutamate accumulation triggers intracellular calcium overload, which may activate DAPK1 and promote its interaction with GluN2B at extrasynaptic sites, resulting in neurotoxicity.^{19,54} Previous studies reported that the blockade of GluN2B-containing NMDARs prevented glutamate accumulation-induced neurotoxicity and even reversed the downregulation of neurotrophic factors.^{19,28,55–57} Rapid-acting antidepressants (for example, NMDAR antagonists) antagonize inhibitory interneurons in the mPFC, leading to the disinhibition of pyramidal neurons and an increase in synaptic glutamate release and recycling, which are capable of increasing α -amino-3-hydroxy-5-methyl-4-isoxazolepropionic acid receptor-mediated neurotransmission and initiating a cascade of events that ultimately facilitate an antidepressant response.^{58–60}

Ifenprodil is an $\alpha 1$ adrenergic receptor antagonist that was originally developed as a vasodilator.⁶¹ It was subsequently found to be a highly selective antagonist of the NMDA GluN2B subunit.⁶² Upon ifenprodil binding, the bi-lobed structure of the GluN2 amino-terminal domain adopts a closed conformation, accompanied by rearrangement of the GluN1–GluN2 amino-terminal domain heterodimeric interface to inhibit receptor activity.^{63,64} In the present study, we found that selective inhibition of the GluN2B subunit with ifenprodil produced rapid antidepressant-like actions in rats that were subjected to the FST and CUS. The inhibition of DAPK1 or its interaction with the GluN2B subunit in the mPFC also exerted rapid and sustained antidepressant-like effects. These behavioral responses were correlated with decreases in the levels of DAPK1 and p-GluN2B, and increases in the levels of p-CREB and BDNF in the mPFC. Extrasynaptic NMDAR stimulation triggers the CREB shut-off pathway, which reduces BDNF expression.^{17,28} The synaptic and behavioral actions of rapid-acting antidepressants require BDNF signaling, which regulates synaptic protein synthesis.^{10,58,65} Thus, the most reasonable explanation for our findings is that under conditions of depression, activated DAPK1 is recruited to the NMDAR GluN2B subunit and phosphorylates the GluN2B subunit at Ser1303, subsequently triggering the CREB shut-off pathway. The inhibition of DAPK1 or GluN2B or their interaction blocked the activation of the CREB shut-off pathway and promoted CREB-dependent gene expression, generating rapid antidepressant-like effects.

Although several studies have shown that the GluN2A subunit is involved in regulating depressive-like behavior,^{21,42} we found that the selective GluN2A antagonist PEAQX at a dose of 5 mg kg⁻¹ had no effect on CUS-induced depressive-like behavior. The distinct roles of GluN2A- and GluN2B-containing NMDARs in the central nervous system have been widely reported, which could explain why GluN2A antagonism did not produce rapid antidepressant-like effects but GluN2B antagonism did.^{14,57,66,67} However, we cannot completely exclude the possibly important role of the GluN2A subunit in the etiology of depression and antidepressant-like effects. The full dose–response effect of the GluN2A antagonist and additional phosphorylation sites of GluN2A need to be studied. A recent study found that the antidepressant-like effects of GluN2B antagonist were absent in *GluN2A* knockout mice, indicating that GluN2A is required for the ability of GluN2B antagonist to reverse depressive-like behavior.²³ Further investigations of the specific roles of the GluN2A and GluN2B subunits in depression are needed.

Recent meta-analyses showed that ketamine, but less so of other NMDAR antagonists, has rapid and prolonged antidepressant efficacy in major depressive disorder and bipolar depressed patients.^{68,69} It is noteworthy to discuss the potential mechanisms that may contribute to the discrepancy between the efficacy of ketamine and other NMDAR antagonists in clinical trials. Although ketamine is a high-affinity NMDA receptor antagonist, it has both opiate and stimulant effects.⁷⁰ Actions on dopaminergic and serotonergic systems and sigma receptors have also been

postulated to be alternate mechanisms of ketamine's antidepressant effects.^{71–75} In addition, the structure and physiology of NMDA receptors are complex. Therefore, different NMDAR antagonists (for example, ketamine and memantine) may have different effects on NMDAR-mediated neurotransmission and downstream intracellular signaling.⁷⁶ Finally, recent studies argued that NMDAR antagonist may not be the primary mechanism of action for ketamine in depression. Ketamine may accumulate in neurons via classic acid trapping in intracellular organelles and directly act on intracellular targets in lysosomes or the endoplasmic reticulum in an NMDAR-independent pathway.^{77–79} The ketamine metabolite (2*R*,6*R*)-hydroxynorketamine exerted rapid and sustained antidepressant effects in mice, although hydroxynorketamine did not affect NMDARs in CA1 hippocampal slices.⁸⁰ In the present study, we found that the DAPK1 interaction with GluN2B in the mPFC has a crucial role in the etiology of depression, and targeting this process produced rapid and sustained antidepressant-like effects. The selective GluN2B-containing NMDAR antagonist ifenprodil did not produce rewarding effects. We propose a model that depicts the involvement of GluN2B-containing NMDARs and associated signaling molecules in the mPFC in depression (Figure 5h).

CONCLUSION

In summary, the present findings support the hypothesis that the DAPK1 interaction with GluN2B in the mPFC has a critical role in the pathophysiology of depression. We found that chronic stress-induced extracellular glutamate accumulation that overflowed onto extrasynaptic GluN2B-containing NMDARs enhanced the DAPK1 interaction with GluN2B and inhibited the downstream CREB–BDNF pathway, all of which contributed to the behavioral symptoms of depression. The selective inhibition of DAPK1 or its interaction with the GluN2B subunit in the mPFC had rapid and sustained antidepressant-like effects. These findings extend our understanding of the glutamatergic mechanisms of depression and antidepressant action, providing novel targets for the development of rapid-acting therapeutic agents with limited side effects.

CONFLICT OF INTEREST

The authors declare no conflict of interest.

ACKNOWLEDGMENTS

This work was supported in part by the National Basic Research Program of China (no. 2015CB856400 and 2015CB553503) and Natural Science Foundation of China (no. 81521063, 31230033, 91432303 and 81171251).

REFERENCES

- Ruengorn C, Sanichwankul K, Niwatananun W, Mahatnirunkul S, Pumpaisalchai W, Patumanond J. Factors related to suicide attempts among individuals with major depressive disorder. *Int J Gen Med* 2012; **5**: 323–330.
- Moussavi S, Chatterji S, Verdes E, Tandon A, Patel V, Ustun B. Depression, chronic diseases, and decrements in health: results from the World Health Surveys. *Lancet* 2007; **370**: 851–858.
- Levine J, Panchalingam K, Rapoport A, Gershon S, McClure RJ, Pettegrew JW. Increased cerebrospinal fluid glutamine levels in depressed patients. *Biol Psychiatry* 2000; **47**: 586–593.
- Hashimoto K, Sawa A, Iyo M. Increased levels of glutamate in brains from patients with mood disorders. *Biol Psychiatry* 2007; **62**: 1310–1316.
- Raudensky J, Yamamoto BK. Effects of chronic unpredictable stress and methamphetamine on hippocampal glutamate function. *Brain Res* 2007; **1135**: 129–135.
- Rial D, Lemos C, Pinheiro H, Duarte JM, Goncalves FQ, Real JI et al. Depression as a glial-based synaptic dysfunction. *Front Cell Neurosci* 2016; **9**: 521.

- 7 Murphy-Royal C, Dupuis J, Groc L, Oliet SH. Astroglial glutamate transporters in the brain: regulating neurotransmitter homeostasis and synaptic transmission. *J Neurosci Res* 2017; e-pub ahead of print 2 February 2017; doi:10.1002/jnr.24029.
- 8 Chowdhury GM, Zhang J, Thomas M, Banasr M, Ma X, Pittman B et al. Transiently increased glutamate cycling in rat PFC is associated with rapid onset of antidepressant-like effects. *Mol Psychiatry* 2017; **22**: 120–126.
- 9 Ghasemi M, Phillips C, Trillo L, De Miguel Z, Das D, Salehi A. The role of NMDA receptors in the pathophysiology and treatment of mood disorders. *Neurosci Biobehav Rev* 2014; **47**: 336–358.
- 10 Duman RS, Voleti B. Signaling pathways underlying the pathophysiology and treatment of depression: novel mechanisms for rapid-acting agents. *Trends Neurosci* 2012; **35**: 47–56.
- 11 Hashimoto K. Emerging role of glutamate in the pathophysiology of major depressive disorder. *Brain Res Rev* 2009; **61**: 105–123.
- 12 Vyklícký V, Korinek M, Smejkalová T, Balik A, Krausová B, Kaniakova M et al. Structure, function, and pharmacology of NMDA receptor channels. *Physiol Res* 2014; **63**: S191–S203.
- 13 Mayer ML, Armstrong N. Structure and function of glutamate receptor ion channels. *Annu Rev Physiol* 2004; **66**: 161–181.
- 14 Vanhoutte P, Bading H. Opposing roles of synaptic and extrasynaptic NMDA receptors in neuronal calcium signalling and BDNF gene regulation. *Curr Opin Neurobiol* 2003; **13**: 366–371.
- 15 Hardingham GE, Bading H. Synaptic versus extrasynaptic NMDA receptor signalling: implications for neurodegenerative disorders. *Nat Rev Neurosci* 2010; **11**: 682–696.
- 16 Liu L, Wong TP, Pozza MF, Lingenhoehl K, Wang Y, Sheng M et al. Role of NMDA receptor subtypes in governing the direction of hippocampal synaptic plasticity. *Science* 2004; **304**: 1021–1024.
- 17 Parsons MP, Raymond LA. Extrasynaptic NMDA receptor involvement in central nervous system disorders. *Neuron* 2014; **82**: 279–293.
- 18 Talantova M, Sanz-Blasco S, Zhang X, Xia P, Akhtar MW, Okamoto S et al. β induces astrocytic glutamate release, extrasynaptic NMDA receptor activation, and synaptic loss. *Proc Natl Acad Sci USA* 2013; **110**: E2518–E2527.
- 19 Tu W, Xu X, Peng L, Zhong X, Zhang W, Soundarapandian MM et al. DAPK1 interaction with NMDA receptor NR2B subunits mediates brain damage in stroke. *Cell* 2010; **140**: 222–234.
- 20 Okamoto S, Pouladi MA, Talantova M, Yao D, Xia P, Ehrnhoefer DE et al. Balance between synaptic versus extrasynaptic NMDA receptor activity influences inclusions and neurotoxicity of mutant huntingtin. *Nat Med* 2009; **15**: 1407–1413.
- 21 Boyce-Rustay JM, Holmes A. Genetic inactivation of the NMDA receptor NR2A subunit has anxiolytic- and antidepressant-like effects in mice. *Neuropsychopharmacology* 2006; **31**: 2405–2414.
- 22 Miller OH, Yang L, Wang CC, Hargroder EA, Zhang Y, Delpire E et al. GluN2B-containing NMDA receptors regulate depression-like behavior and are critical for the rapid antidepressant actions of ketamine. *Elife* 2014; **3**: e03581.
- 23 Kiselycznyk C, Jury NJ, Halladay LR, Nakazawa K, Mishina M, Sprengel R et al. NMDA receptor subunits and associated signaling molecules mediating antidepressant-related effects of NMDA-GluN2B antagonism. *Behav Brain Res* 2015; **287**: 89–95.
- 24 Brown DG, Maier DL, Sylvester MA, Hoerter TN, Menhaji-Klotz E, Lasota CC et al. 2,6-Disubstituted pyrazines and related analogs as NR2B site antagonists of the NMDA receptor with anti-depressant activity. *Bioorg Med Chem Lett* 2011; **21**: 3399–3403.
- 25 Ibrahim L, Diaz Granados N, Jolkovsky L, Brutsche N, Luckenbaugh DA, Herring WJ et al. A randomized, placebo-controlled, crossover pilot trial of the oral selective NR2B antagonist MK-0657 in patients with treatment-resistant major depressive disorder. *J Clin Psychopharmacol* 2012; **32**: 551–557.
- 26 Preskorn SH, Baker B, Kolluri S, Menniti FS, Krams M, Landen JW. An innovative design to establish proof of concept of the antidepressant effects of the NR2B subunit selective N-methyl-D-aspartate antagonist, CP-101,606, in patients with treatment-refractory major depressive disorder. *J Clin Psychopharmacol* 2008; **28**: 631–637.
- 27 Krupp JJ, Vissel B, Thomas CG, Heinemann SF, Westbrook GL. Interactions of calmodulin and α -actinin with the NR1 subunit modulate Ca^{2+} -dependent inactivation of NMDA receptors. *J Neurosci* 1999; **19**: 1165–1178.
- 28 Hardingham GE, Fukunaga Y, Bading H. Extrasynaptic NMDARs oppose synaptic NMDARs by triggering CREB shut-off and cell death pathways. *Nat Neurosci* 2002; **5**: 405–414.
- 29 Ma YY, Yu P, Guo CY, Cui CL. Effects of ifenprodil on morphine-induced conditioned place preference and spatial learning and memory in rats. *Neurochem Res* 2011; **36**: 383–391.
- 30 John CS, Smith KL, Van't Veer A, Gompf HS, Carlezon WA Jr, Cohen BM et al. Blockade of astrocytic glutamate uptake in the prefrontal cortex induces anhedonia. *Neuropsychopharmacology* 2012; **37**: 2467–2475.
- 31 Okamoto M, Takayama K, Shimizu T, Ishida K, Takahashi O, Furuya T. Identification of death-associated protein kinase inhibitors using structure-based virtual screening. *J Med Chem* 2009; **52**: 7323–7327.
- 32 Shi HS, Zhu WL, Liu JF, Luo YX, Si JJ, Wang SJ et al. PI3K/Akt signaling pathway in the basolateral amygdala mediates the rapid antidepressant-like effects of trefoil factor 3. *Neuropsychopharmacology* 2012; **37**: 2671–2683.
- 33 Zhu WL, Wang SJ, Liu MM, Shi HS, Zhang RX, Liu JF et al. Glycine site N-methyl-D-aspartate receptor antagonist 7-CTKA produces rapid antidepressant-like effects in male rats. *J Psychiatry Neurosci* 2013; **38**: 306–316.
- 34 Banasr M, Duman RS. Glial loss in the prefrontal cortex is sufficient to induce depressive-like behaviors. *Biol Psychiatry* 2008; **64**: 863–870.
- 35 Trantham-Davidson H, LaLumiere RT, Reissner KJ, Kalivas PW, Knackstedt LA. Ceftriaxone normalizes nucleus accumbens synaptic transmission, glutamate transport, and export following cocaine self-administration and extinction training. *J Neurosci* 2012; **32**: 12406–12410.
- 36 Zhang Y, Xue Y, Meng S, Luo Y, Liang J, Li J et al. Inhibition of lactate transport erases drug memory and prevents drug relapse. *Biol Psychiatry* 2016; **79**: 928–939.
- 37 Li N, Lee B, Liu RJ, Banasr M, Dwyer JM, Iwata M et al. mTOR-dependent synapse formation underlies the rapid antidepressant effects of NMDA antagonists. *Science* 2010; **329**: 959–964.
- 38 Han Y, Luo Y, Sun J, Ding Z, Liu J, Yan W et al. AMPK signaling in the dorsal hippocampus negatively regulates contextual fear memory formation. *Neuropsychopharmacology* 2016; **41**: 1849–1864.
- 39 Zhang RX, Han Y, Chen C, Xu LZ, Li JL, Chen N et al. EphB2 in the medial prefrontal cortex regulates vulnerability to stress. *Neuropsychopharmacology* 2016; **41**: 2541–2556.
- 40 Arnth-Jensen N, Jabaudon D, Scanziani M. Cooperation between independent hippocampal synapses is controlled by glutamate uptake. *Nat Neurosci* 2002; **5**: 325–331.
- 41 Shen HW, Scofield MD, Boger H, Hensley M, Kalivas PW. Synaptic glutamate spillover due to impaired glutamate uptake mediates heroin relapse. *J Neurosci* 2014; **34**: 5649–5657.
- 42 Taniguchi S, Nakazawa T, Tanimura A, Kiyama Y, Tezuka T, Watabe AM et al. Involvement of NMDAR_{2A} tyrosine phosphorylation in depression-related behaviour. *EMBO J* 2009; **28**: 3717–3729.
- 43 Danbolt NC. Glutamate uptake. *Prog Neurobiol* 2001; **65**: 1–105.
- 44 Cotter D, Mackay D, Landau S, Kerwin R, Everall I. Reduced glial cell density and neuronal size in the anterior cingulate cortex in major depressive disorder. *Arch Gen Psychiatry* 2001; **58**: 545–553.
- 45 Zink M, Vollmayr B, Gebicke-Haerter PJ, Henn FA. Reduced expression of glutamate transporters vGluT1, EAAT2 and EAAT4 in learned helpless rats, an animal model of depression. *Neuropharmacology* 2010; **58**: 465–473.
- 46 Bowley MP, Drevets WC, Ongur D, Price JL. Low glial numbers in the amygdala in major depressive disorder. *Biol Psychiatry* 2002; **52**: 404–412.
- 47 Sapolsky RM. The possibility of neurotoxicity in the hippocampus in major depression: a primer on neuron death. *Biol Psychiatry* 2000; **48**: 755–765.
- 48 Mauri MC, Ferrara A, Boscati L, Bravin S, Zamberlan F, Alecci M et al. Plasma and platelet amino acid concentrations in patients affected by major depression and under fluoxetine treatment. *Neuropsychobiology* 1998; **37**: 124–129.
- 49 Brassai A, Suvanjev RG, Ban EG, Lakatos M. Role of synaptic and nonsynaptic glutamate receptors in ischaemia induced neurotoxicity. *Brain Res Bull* 2015; **112**: 1–6.
- 50 Petralia RS. Distribution of extrasynaptic NMDA receptors on neurons. *ScientificWorldJournal* 2012; **2012**: 267120.
- 51 Pal B. Astrocytic actions on extrasynaptic neuronal currents. *Front Cell Neurosci* 2015; **9**: 474.
- 52 Gerhard DM, Wohleb ES, Duman RS. Emerging treatment mechanisms for depression: focus on glutamate and synaptic plasticity. *Drug Discov Today* 2016; **21**: 454–464.
- 53 Shohat G, Spivak-Kroizman T, Cohen O, Bialik S, Shani G, Berrisi H et al. The pro-apoptotic function of death-associated protein kinase is controlled by a unique inhibitory autophosphorylation-based mechanism. *J Biol Chem* 2001; **276**: 47460–47467.
- 54 Lipton SA. Paradigm shift in neuroprotection by NMDA receptor blockade: memantine and beyond. *Nat Rev Drug Discov* 2006; **5**: 160–170.
- 55 Li N, Liu RJ, Dwyer JM, Banasr M, Lee B, Son H et al. Glutamate N-methyl-D-aspartate receptor antagonists rapidly reverse behavioral and synaptic deficits caused by chronic stress exposure. *Biol Psychiatry* 2011; **69**: 754–761.
- 56 Vizi ES, Kisfalvi M, Lorincz T. Role of nonsynaptic GluN2B-containing NMDA receptors in excitotoxicity: evidence that fluoxetine selectively inhibits these receptors and may have neuroprotective effects. *Brain Res Bull* 2013; **93**: 32–38.
- 57 Kaufman AM, Milnerwood AJ, Sepers MD, Coquinco A, She K, Wang L et al. Opposing roles of synaptic and extrasynaptic NMDA receptor signaling in cocultured striatal and cortical neurons. *J Neurosci* 2012; **32**: 3992–4003.

- 58 Autry AE, Adachi M, Nosyreva E, Na ES, Los MF, Cheng PF *et al*. NMDA receptor blockade at rest triggers rapid behavioural antidepressant responses. *Nature* 2011; **475**: 91–95.
- 59 Wohleb ES, Gerhard D, Thomas A, Duman RS. Molecular and cellular mechanisms of rapid-acting antidepressants ketamine and scopolamine. *Curr Neuropharmacol* 2017; **15**: 11–20.
- 60 Cornwell BR, Salvatore G, Furey M, Marquardt CA, Brutsche NE, Grillon C *et al*. Synaptic potentiation is critical for rapid antidepressant response to ketamine in treatment-resistant major depression. *Biol Psychiatry* 2012; **72**: 555–561.
- 61 Young AR, Bouloy M, Boussard JF, Edvinsson L, MacKenzie ET. Direct vascular effects of agents used in the pharmacotherapy of cerebrovascular disease on isolated cerebral vessels. *J Cereb Blood Flow Metab* 1981; **1**: 117–128.
- 62 Williams K. Ifenprodil discriminates subtypes of the N-methyl-D-aspartate receptor: selectivity and mechanisms at recombinant heteromeric receptors. *Mol Pharmacol* 1993; **44**: 851–859.
- 63 Tajima N, Karakas E, Grant T, Simorowski N, Diaz-Avalos R, Grigorieff N *et al*. Activation of NMDA receptors and the mechanism of inhibition by ifenprodil. *Nature* 2016; **534**: 63–68.
- 64 Karakas E, Simorowski N, Furukawa H. Subunit arrangement and phenylethanolamine binding in GluN1/GluN2B NMDA receptors. *Nature* 2011; **475**: 249–253.
- 65 Duman RS, Aghajanian GK. Synaptic dysfunction in depression: potential therapeutic targets. *Science* 2012; **338**: 68–72.
- 66 Liu Y, Wong TP, Aarts M, Rooyakkers A, Liu L, Lai TW *et al*. NMDA receptor subunits have differential roles in mediating excitotoxic neuronal death both in vitro and in vivo. *J Neurosci* 2007; **27**: 2846–2857.
- 67 Massey PV, Johnson BE, Moulton PR, Auberson YP, Brown MW, Molnar E *et al*. Differential roles of NR2A and NR2B-containing NMDA receptors in cortical long-term potentiation and long-term depression. *J Neurosci* 2004; **24**: 7821–7828.
- 68 Newport DJ, Carpenter LL, McDonald WM, Potash JB, Tohen M, Nemeroff CB *et al*. Ketamine and other NMDA antagonists: early clinical trials and possible mechanisms in depression. *Am J Psychiatry* 2015; **172**: 950–966.
- 69 Kishimoto T, Chawla JM, Hagi K, Zarate CA, Kane JM, Bauer M *et al*. Single-dose infusion ketamine and non-ketamine N-methyl-D-aspartate receptor antagonists for unipolar and bipolar depression: a meta-analysis of efficacy, safety and time trajectories. *Psychol Med* 2016; **46**: 1459–1472.
- 70 Elliott K, Kest B, Man A, Kao B, Inturrisi CE. N-methyl-D-aspartate (NMDA) receptors, mu and kappa opioid tolerance, and perspectives on new analgesic drug development. *Neuropsychopharmacology* 1995; **13**: 347–356.
- 71 Tan S, Lam WP, Wai MS, Yu WH, Yew DT. Chronic ketamine administration modulates midbrain dopamine system in mice. *PLoS One* 2012; **7**: e43947.
- 72 Lindfors N, Barati S, O'Connor WT. Differential effects of single and repeated ketamine administration on dopamine, serotonin and GABA transmission in rat medial prefrontal cortex. *Brain Res* 1997; **759**: 205–212.
- 73 Gigliucci V, O'Dowd G, Casey S, Egan D, Gibney S, Harkin A. Ketamine elicits sustained antidepressant-like activity via a serotonin-dependent mechanism. *Psychopharmacology (Berl)* 2013; **228**: 157–166.
- 74 Belujon P, Grace AA. Restoring mood balance in depression: ketamine reverses deficit in dopamine-dependent synaptic plasticity. *Biol Psychiatry* 2014; **76**: 927–936.
- 75 Robson MJ, Elliott M, Seminerio MJ, Matsumoto RR. Evaluation of sigma (sigma) receptors in the antidepressant-like effects of ketamine in vitro and in vivo. *Eur Neuropsychopharmacol* 2012; **22**: 308–317.
- 76 Gideons ES, Kavalali ET, Monteggia LM. Mechanisms underlying differential effectiveness of memantine and ketamine in rapid antidepressant responses. *Proc Natl Acad Sci USA* 2014; **111**: 8649–8654.
- 77 Lester HA, Lavis LD, Dougherty DA. Ketamine inside neurons? *Am J Psychiatry* 2015; **172**: 1064–1066.
- 78 Lester HA, Miwa JM, Srinivasan R. Psychiatric drugs bind to classical targets within early exocytotic pathways: therapeutic effects. *Biol Psychiatry* 2012; **72**: 907–915.
- 79 Baker SC, Shabir S, Georgopoulos NT, Southgate J. Ketamine-induced apoptosis in normal human urothelial cells: a direct, N-methyl-D-aspartate receptor-independent pathway characterized by mitochondrial stress. *Am J Pathol* 2016; **186**: 1267–1277.
- 80 Zanos P, Moaddel R, Morris PJ, Georgiou P, Fischell J, Elmer GI *et al*. NMDAR inhibition-independent antidepressant actions of ketamine metabolites. *Nature* 2016; **533**: 481–486.



This work is licensed under a Creative Commons Attribution-NonCommercial-NoDerivs 4.0 International License. The images or other third party material in this article are included in the article's Creative Commons license, unless indicated otherwise in the credit line; if the material is not included under the Creative Commons license, users will need to obtain permission from the license holder to reproduce the material. To view a copy of this license, visit <http://creativecommons.org/licenses/by-nc-nd/4.0/>

© The Author(s) 2018

Supplementary Information accompanies the paper on the Molecular Psychiatry website (<http://www.nature.com/mp>)